



Simulation Analysis of Induction Heating as a Self-Healing Method on Asphalt

Ardi Esdiyanto¹, Ubaidillah^{1,*}, Eko Prasetya Budiana¹, Senot Sangadji², Bhre Wangsa Lenggana¹

¹ Department of Mechanical Engineering, Faculty of Engineering, Universitas Sebelas Maret, Surakarta 57126, Indonesia

² Department of Civil Engineering, Faculty of Engineering, Universitas Sebelas Maret, Surakarta 57126, Indonesia

ARTICLE INFO

Article history:

Received 20 July 2022

Received in revised form 21 August 2022

Accepted 19 October 2022

Available online 1 March 2023

Keywords:

Induction Heating; Self-Healing Asphalt;
Induction Heating Simulation

ABSTRACT

Asphalt is a self-healing material at a specific temperature. The induced heating-healing of asphalt has been developed in the last few decades; an inductive asphalt can be created by adding inductive material. This paper aims to predict the performance of induction heating as a self-healing method on asphalt. This numerical simulation is carried out to obtain a suitable induction heater configuration. Numerical simulation is carried out in two stages, electrical analysis with ANSYS Electronics Desktop software and thermal analysis with ANSYS Transient Thermal Analysis. A cylindrical inductive asphalt sample is modeled and subjected to an electromagnetic field by a coil flowed by a high-frequency AC. As a result, a comparative temperature distribution is obtained by several current and frequency variations. The difference in current magnitude and frequency that flowed in the coil affects asphalt's heating performance and healing capacity. An increase in the frequency configuration results in a more significant increase in temperature than increasing the current magnitude in the coil.

1. Introduction

Asphalt is the most used pavement type in the world, and it has several advantages such as noise reduction, comfortable driving experience, and cost-efficiency [1-3]. Asphalt roads have become the main part of the transportation system and human life development. The asphalt road network in Indonesia is estimated to be 516,239 kilometers long. It has become the main role in goods trading and regional economic development [4]. Every day, asphalt is continuously exposed to various environmental effects such as rain, chemical fluids, road loads, and varying temperatures that will damage the surface of the asphalt. As time goes on, the asphalt will begin to crack and cause water to enter through the cracks that appear [5]. During the last few decades, efforts to reduce the use of non-renewable natural resources to protect the environment have increased, especially in the automotive sector and its supporting facilities [6].

Self-healing material can be defined as the ability of a material to heal itself from existing damage without any external intervention. The goal of self-healing is to reduce the level of damage and

* Corresponding author.

E-mail address: ubaidillah_ft@staff.uns.ac.id (Ubaidillah)

extend the service life [7]. As shown in Figure 1, conventional material accumulates damage and will fail after a certain time. While the improvised material has the same principle, there is only a short additional service life. Whereas self-healing materials may do some minor damage at first but will extend their service life significantly until they reach total damage and cannot be used more [8].

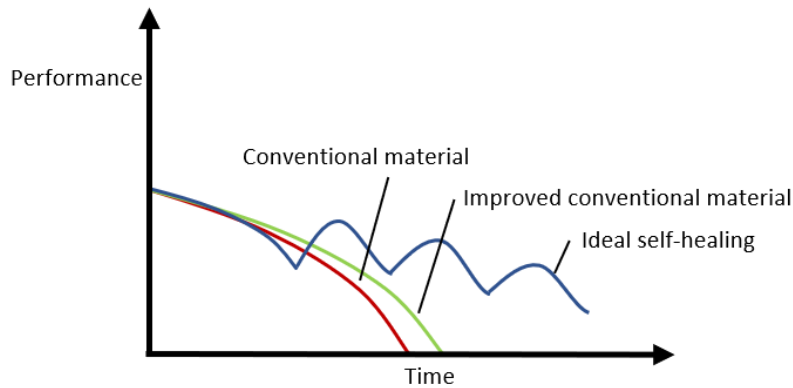


Fig. 1. The behavior of the material with time

Since 1960, the self-healing asphalt ability has been researched in several labs. Researchers believe that closing the microcrack can extend the service life of the asphalt [9,10]. Asphalt can repair the damage by itself, but it needs certain conditions such as resting from any road load and at a specific temperature [11]. Several studies have shown that temperature is the most important factor in accelerating healing performance [12-15]. The self-healing on asphalt works because the viscosity property of asphalt is inversely proportional to temperature [5,16]. Although asphalt fluid material is a non-newtonian fluid, it can be a Newtonian fluid at a specific temperature (around 70 °C). At this moment, asphalt or bitumen can flow with the effect of gravity and fill cracks or gaps in a capillary flow [17-19]. While the optimum temperature for self-healing is 85 °C, the excessive temperature will reduce the asphalt healing ratio [13]. Various methods have been studied to achieve the self-healing phase of asphalt, such as encapsulated rejuvenators [20], microvascular fibers [21], microwave heating [22], and induction heating [23].

Liu [13] has performed a comparative study using three types of steel fiber with various diameters. Asphalt diameters (29.6 – 191.1 μm , 8.89 – 12.7 μm , and 6.38 – 8.89 μm). Porous asphalt samples with 100 mm diameter and 50 mm thickness were heated with a 50-kW induction heater with a frequency of 70 kHz. The setup that is used is shown in Figure 2. It was observed that steel fibers with longer lengths but smaller diameters have better heating performance than shorter lengths and larger diameters. This is due to the contact between the fibers is tighter and results in higher electrical conductivity. Liu [13] also concluded that the porous asphalt concrete had improved fatigue resistance and healing capacity, which will improve the durability of the asphalt. After reaching 85 °C, the porous asphalt has significantly healed after 3 hours of cooling. The environmental condition also affects the induction heating performance. A day with low wind speed and a high temperature will have a better result [24].



Fig. 2. Induction heating setup [13]

2. Fundamental of Induction Heating on Asphalt

2.1 Induction Heating

Induction heating gives a contactless, fast, and efficient heating process in metal or conductive materials. This technology is one of the most popular heating methods in industrial works. In general, induction heating is generated by converting power in AC-DC-AC. An AC supplies a high-frequency alternating voltage to a working coil [25]. This alternating current will generate a magnetic field around its coil that penetrates the load object. The load object will be heated due to two phenomena, eddy currents and magnetic hysteresis [26]. The induction heating system is assembled by a working coil, a power supply, a converter, and a cooling system, as shown in Figure 3. Coil winding, coil diameter, type of object being heated, the distance between the object and coil, and configuration of the induction heater may affect the generated heat [27].

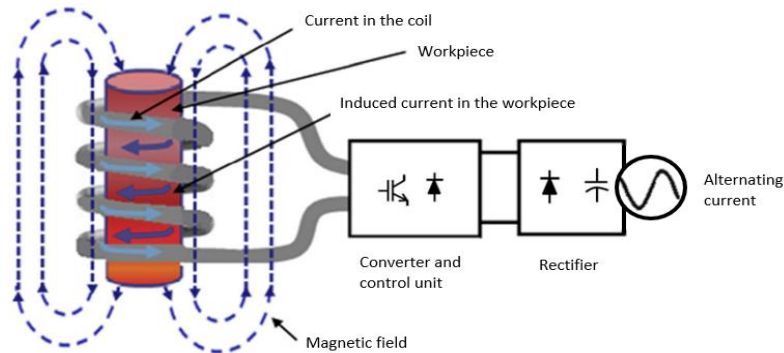


Fig. 3. Main components of induction heating system [27]

The eddy current generated in the workpiece depends on the magnitude of the electromagnetic field created [28]. The equations of electromagnetic induction heating are Maxwell's equations, which can be described as follows:

Ampere's Law

$$\nabla \times \mathbf{H} = \mathbf{J} + \frac{\partial \mathbf{D}}{\partial t} \quad (1)$$

Faraday's Law

$$\nabla \times \mathbf{E} = -\frac{\partial \mathbf{B}}{\partial t} \quad (2)$$

Gauss Law

$$\nabla \cdot \mathbf{B} = 0 \quad (3)$$

Gauss's Law

$$\nabla \cdot \mathbf{D} = \rho \quad (4)$$

where \mathbf{H} is the magnetic field intensity (A/m), \mathbf{J} is the electric current density associated with free charges (A/m²), \mathbf{B} is the magnetic flux density (weber/m²), and \mathbf{E} is the electric field density (V/m). In addition, the parameters \mathbf{H} , \mathbf{J} , \mathbf{B} , and \mathbf{E} follow these equations:

$$\mathbf{B} = \mu_0 \mu_r \mathbf{H} \quad (5)$$

$$\mathbf{D} = \varepsilon_0 \varepsilon_r \mathbf{E} \quad (6)$$

$$\mathbf{J} = \sigma \mathbf{E} \quad (7)$$

$$\sigma = 1/\rho \quad (8)$$

where ε is relative permittivity, μ is magnetic permeability, σ is the material's electrical conductivity, and ρ is electrical resistivity. The permittivity value in a vacuum is expressed by $\varepsilon_0 = 8.854 \times 10^{-7}$ F/m. Meanwhile, permeability states the ability of a material to conduct magnetic flux compared to a vacuum. The value of permeability in a vacuum is expressed by $\mu_0 = 4\pi \times 10^{-7}$ H/m [29].

Induction heating is a process that generates a drastic increase in temperature in a short period, and extreme temperature changes occur on the surface usually happened due to the skin effect. The distribution of temperature of a whole body of workpiece can be expressed by the following Fourier equation:

$$k \left(\frac{\partial^2 T}{\partial x^2} + \frac{\partial^2 T}{\partial y^2} + \frac{\partial^2 T}{\partial z^2} \right) + Q = \rho c \frac{\partial T}{\partial t} \quad (9)$$

where k is the thermal conductivity coefficient, Q is internal heat source intensity due to eddy current, c is the specific heat capacity of the workpiece, and ρ is density [29,30].

2.2 Mechanism of Induction Heating on Asphalt

Heat is a form of energy that passes from higher temperature to lower temperature, heat transfer has played an important role in human life today [31,32]. Meanwhile, the temperature is the most important factor that influences self-healing performance on asphalt, and increasing temperature directly reduces the time needed for asphalt to heal the cracks. To achieve this condition, induced heating-healing was studied and developed by Liu [13]. Induction heating can only be used on conductive materials, and ordinary asphalt is not a conductive material. To solve this problem, conductive materials must be added to the asphalt mixture. Some conductive filler materials can be used, but steel fiber is the most common material used as an addition to increase the overall electricity of the asphalt [13,15,16,33,34]. The systematic overview of the induction healing mechanism is shown in Figure 4.

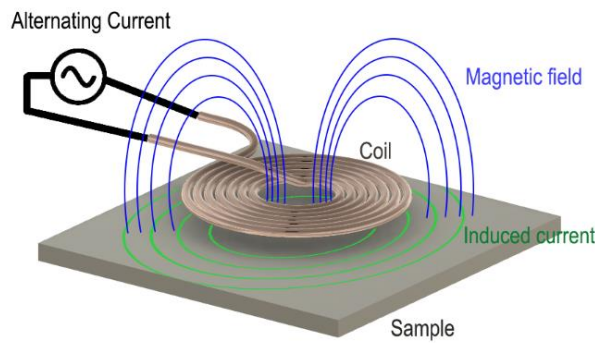


Fig. 4. A systematic overview of induction heating for asphalt

Some additive materials can be used, such as steel fiber and iron powder. Apostolidis [35] conducted that the addition of steel fiber gave a more significant increase in electrical conductivity than iron powder. Using steel fiber also increases tensile strength and extends fatigue life. Apostolidis [35] also mentioned that the efficiency of induction heating increases directly proportional to the concentration of additives, but this addition has a certain limit, whereas the temperature will not increase anymore. The microstructural schematic of the induced healing method is shown in Figure 5.

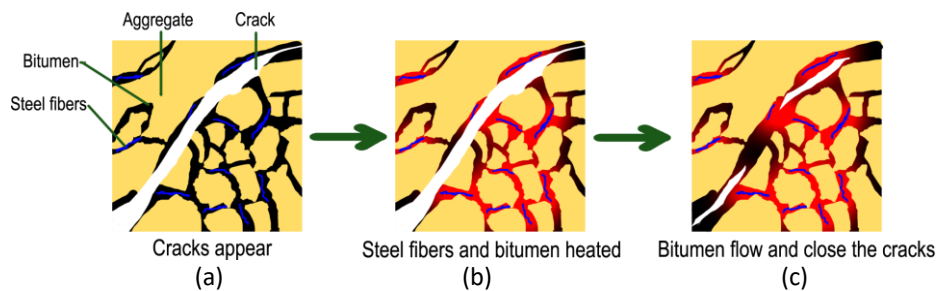


Fig. 5. Microstructural schematic of induced healing method (a) Crack surface (b) Heating process (c) Healing process

3. Methodology

This study was performed by finite element method analysis. As shown in Figure 6, ANSYS Electronics Desktop was used for electrical analysis, and ANSYS Transient Thermal was used for thermal analysis [36,37]. Firstly, the electrical analysis using ANSYS Electronics Desktop was carried out until the desired convergence was obtained, and then the output of this simulation was imported to thermal analysis. After that, thermal analysis was carried out using ANSYS Transient Thermal analysis until convergence data was obtained.

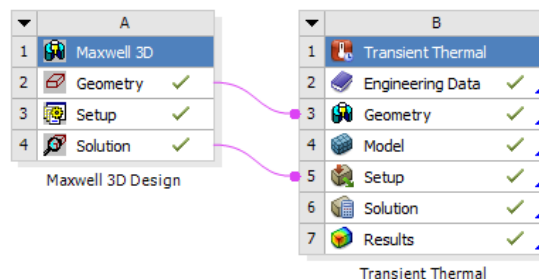


Fig. 6. A schematic process of coupled analysis

The inductive asphalt and working coil are modeled directly using ANSYS Electronics Desktop software. To minimize system memory storage and reduce analysis computation time, the geometrical model of the working coil is simplified. An inductive asphalt sample has been modeled with 100 mm diameter and 60 mm thickness. A hollow copper tube coil has been modeled with 9 turns, 140 mm diameter, 5 mm width, and 0,1 thickness. The coil was placed 2.5 mm at the top of the asphalt to assume that the two surfaces have a small gap, as shown in Figure 7. The properties of inductive asphalt were referenced from a previous study by Apostolidis [35] using 13.27% steel fiber addition. The parameters of this simulation are shown in Table 1.

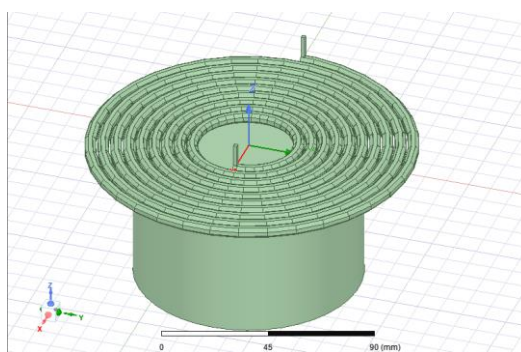


Fig. 7. Inductive asphalt and working coil model

Table 1
 Simulation parameters for electrical analysis

Material	Inductive Asphalt	Copper
Mass density (Kg/m ³)	2360	8933
Relative Permittivity	6	1
Relative Permeability	1	0.999
Bulk Conductivity (S/m)	2100	58000000

The geometry has meshed before the solution. The eddy current solution is used in electrical analysis to obtain ohmic loss data. In this calculation, several variations of current magnitudes and frequencies are applied. The environment of this simulation was set as vacuum volume. The iteration had been carried out by ANSYS until the solution converged. Since the data is directly linked and transferred to the thermal analysis, numerical recording data is unnecessary. However, the data regarding the electromagnetic field and the resulting ohmic loss data are taken to be analyzed in the next step.

After the electrical part was completed, the ANSYS Transient Thermal setup was initiated. Geometry and mesh were carried out from the previous simulation. The converged solution from the electrical analysis is imported as internal heat generation in this process. Several thermal properties are defined here, such as initial and environment temperature are set as 27 °C. In this part, heat loss by radiation was assumed be negligible, there is only convection with natural convection on air. The simulation was set for the first 900s. The temperature distribution data is obtained to be analyzed later. The parameters of thermal analysis are shown in Table 2.

Table 2
 Simulation parameters for thermal analysis [35]

Material	Inductive Asphalt
Mass density (kg/m ³)	2360
Thermal conductivity (W/m·°C)	1,58
Specific heat (J/kg·°C)	920

An experiment was carried out to validate the simulation. An inductive asphalt sample with 14% steel fiber addition is prepared. The sample has 1134 grams of aggregate, with steel fiber addition that has 0.489 gr/cc density. The mass of the mixture of aggregate and asphalt in one module is 1200 grams. The mixing temperature and the mixing time are important parameters for the preparation of the sample. The mixing procedure for the sample was based on the method outlined by Apostolidis [35]. The sample is placed right under the coil until the two surfaces are in contact with each other. But due to the uneven shape of the coil, there is a gap of up to 5 mm on the outside of the coil. A cylindrical sample was used to maximize the induced heating potential that occurs which is supported by the geometry used in the experiment. This sample is heated using a 9 Volt 70 Ampere induction heater with a frequency of 39 kHz. The experimental setup is shown in Figure 8. The first variation of simulation will be compared with the experiment result before continuing to other variations. Slightly different results will be tolerated because the modeling of the boundary conditions cannot be completely identical.

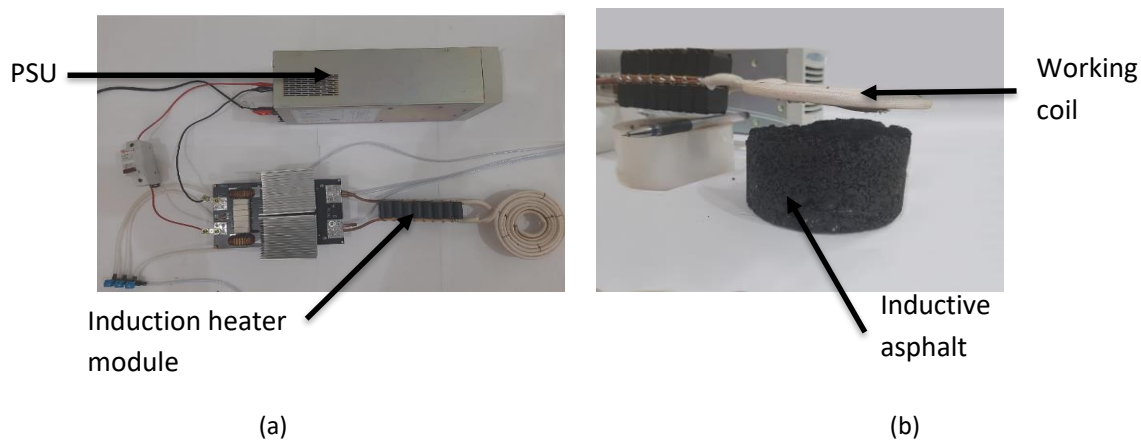


Fig. 8. Induction heating experiment setup (a) top view (b) side view

4. Result

4.1 Electrical Analysis

The electrical analysis aims to obtain electromagnetic field and ohmic loss distribution around the inductive asphalt so that data can be directly used as internal heat generation in thermal analysis to obtain temperature distribution. The comparison of the distribution of electromagnetic fields at frequencies of 39 and 70 kHz at currents of 70 and 200 A can be seen in Figure 9 and Figure 10 below. It can be seen that the electromagnetic field intensity H has a peak value on the center top surface of inductive asphalt. It is because a higher electromagnetic field penetrates the central surface area of inductive asphalt than other areas. The higher current produces a greater electromagnetic field based on Ampere's Law which states that the magnitude of the electromagnetic field is directly proportional to the displacement of the electric charge, where current is the product of the electric charge multiplied by time.

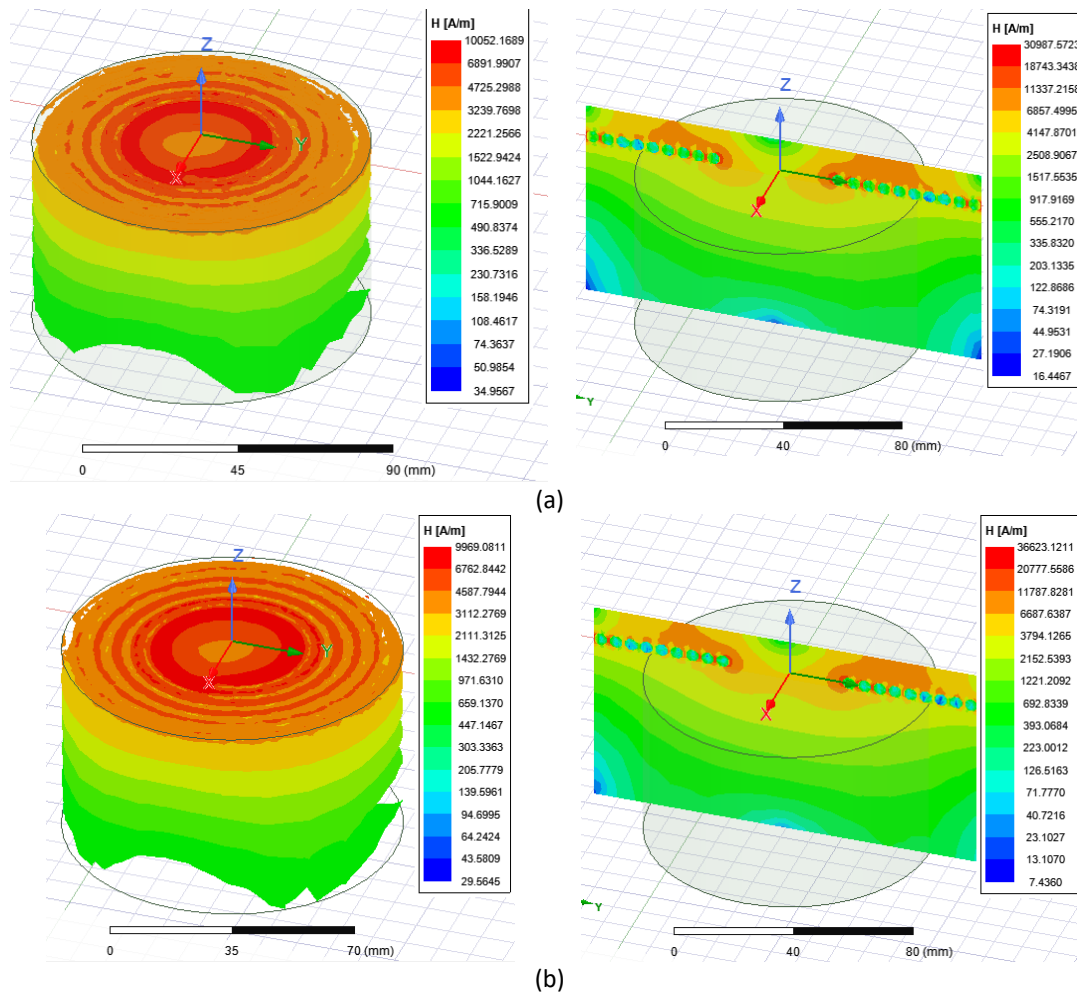
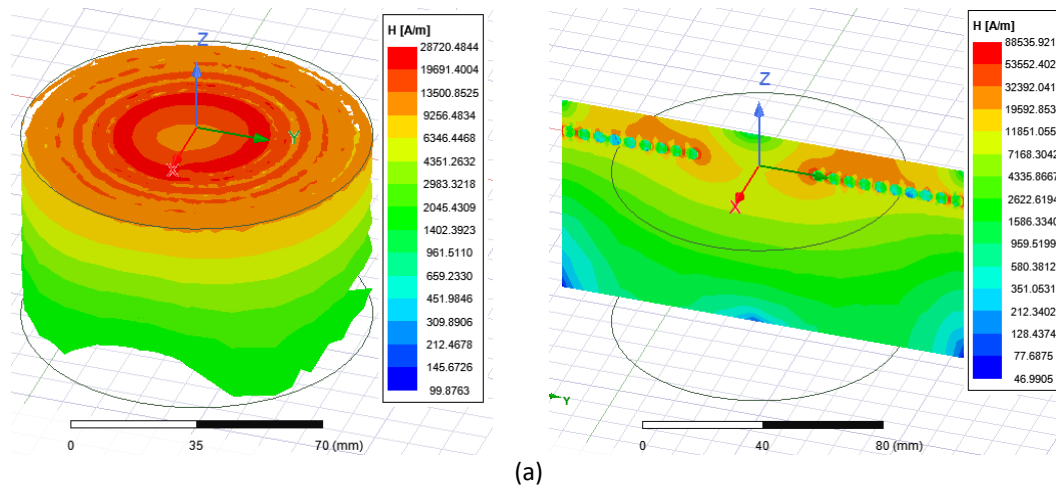


Fig. 9. Comparison of the electromagnetic field on asphalt with a current of 70 A (a) 39 kHz (b) 70 kHz



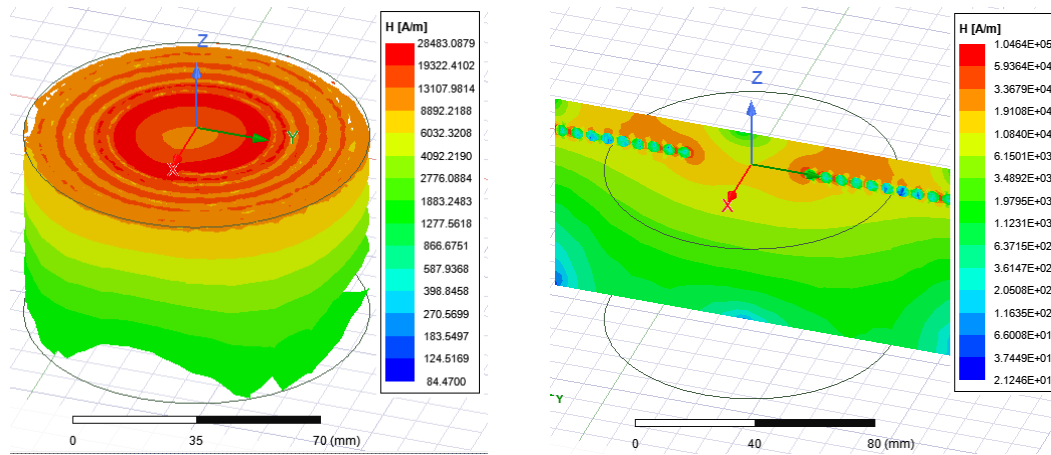


Fig. 10. Comparison of the electromagnetic field on asphalt with a current of 200 A (a) 39 kHz (b) 70 kHz

Figure 11 shows the maximum value of the electromagnetic field generated from all the variations that have been carried out. It is seen that the difference in frequency used does not produce a significant difference for the maximum value of the electromagnetic field. The electromagnetic field increases in proportion to the value of the current that used.

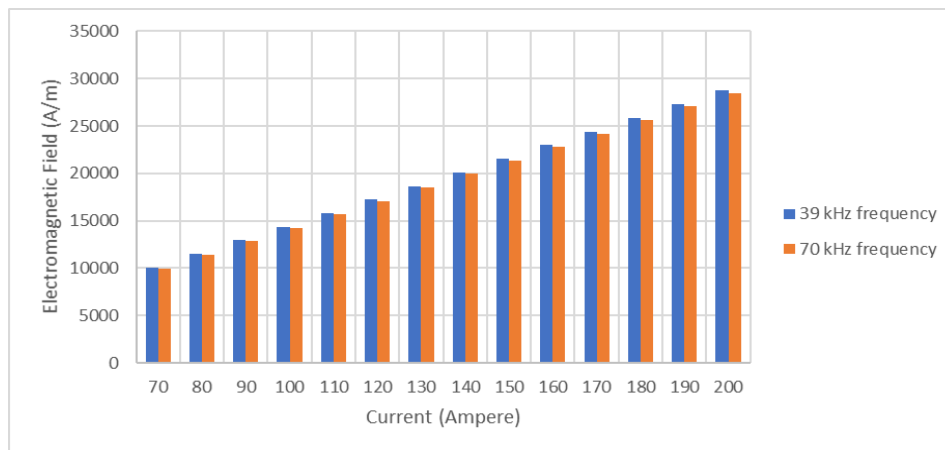


Fig. 11. The maximum value of the electromagnetic field in all variations

Meanwhile, the ohmic loss has been found higher at the outside top surface of inductive asphalt as shown in Figure 12 and Figure 13. This is because the outside area is right under the working coil. It makes the eddy current generated more in this area. The ohmic loss was also getting lower gradually along with its thickness. The ohmic loss will also increase directly proportional to the current and frequency value. Increasing the frequency will increase the possibility of power dissipation in each cycle, the accumulation of this dissipation increases the ohmic losses that occur. This power dissipation which turns into heat is utilized in the induction heating method.

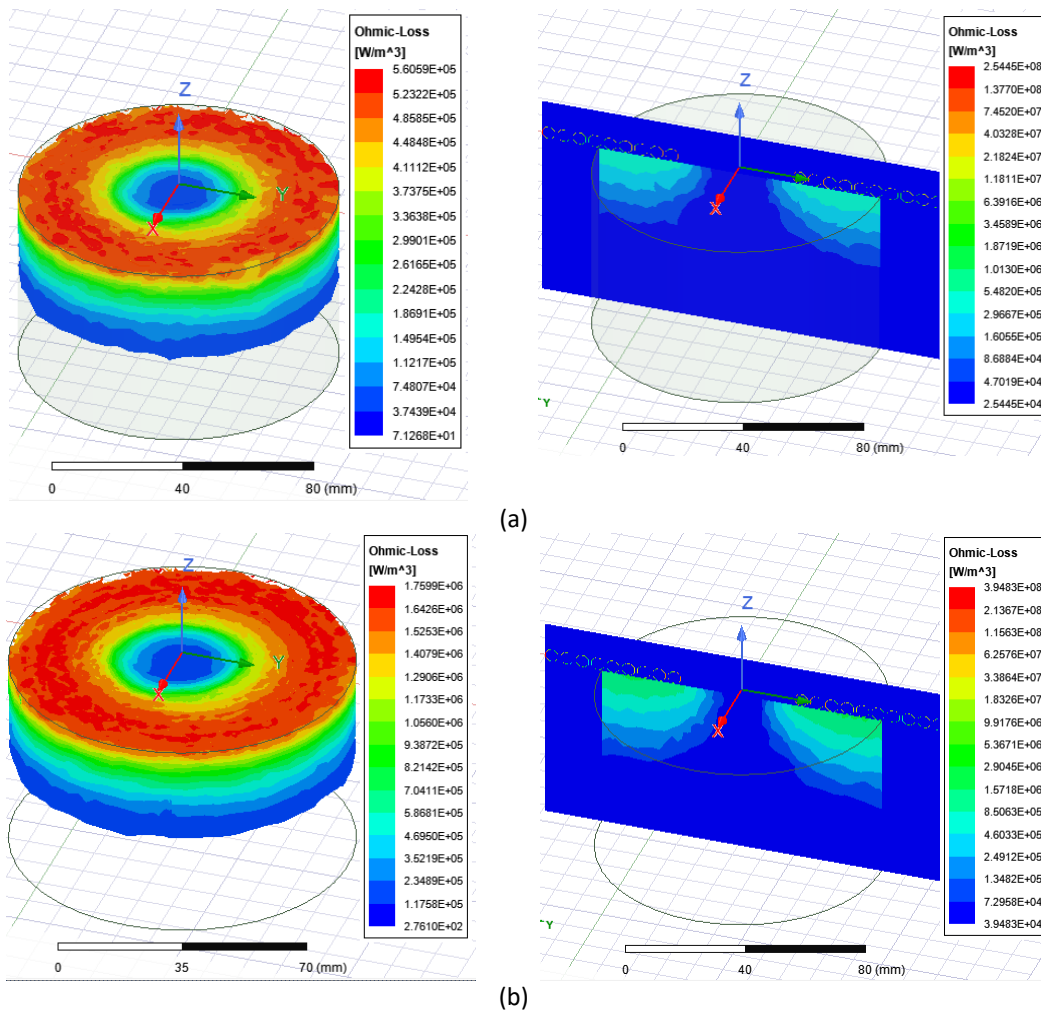
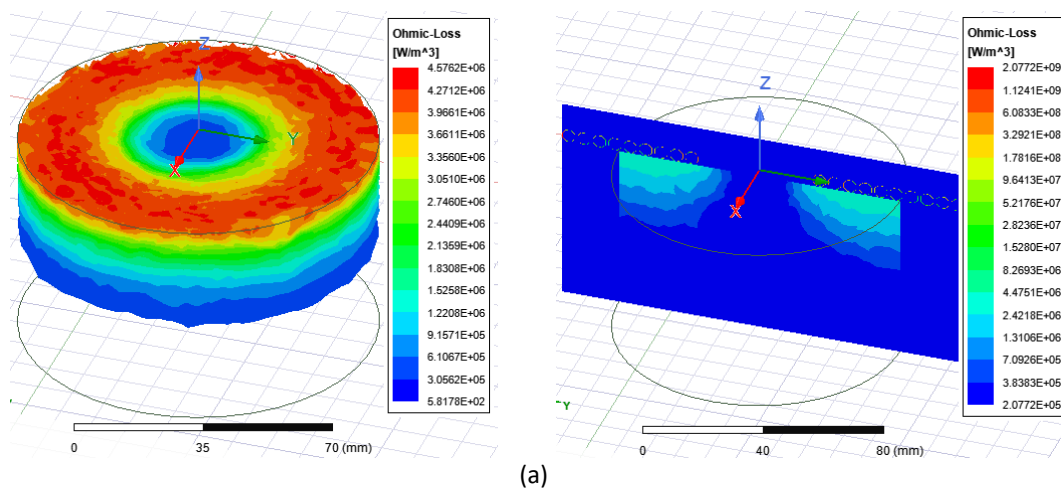


Fig. 12. Comparison of the ohmic loss asphalt with a current of 70 A (a) 39 kHz (b) 70 kHz



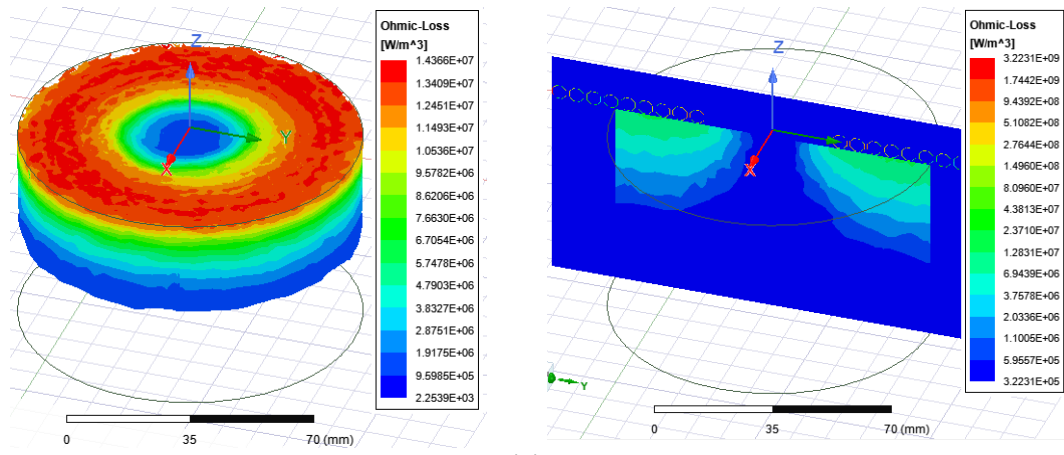


Fig. 13. Comparison of the ohmic loss asphalt with a current of 200 A (a) 39 kHz (b) 70 kHz

Figure 14 shows the maximum ohmic loss that occurs from all the variations that have been done. It can be seen that the peak value of ohmic loss that occurs at the 70 kHz variation is almost three times stronger than the 39 kHz variation. An increase in current also increases the amount of ohmic loss generated. Because the model is not magnetic enough, the heat will be more generated due to ohmic loss than hysteresis loss.

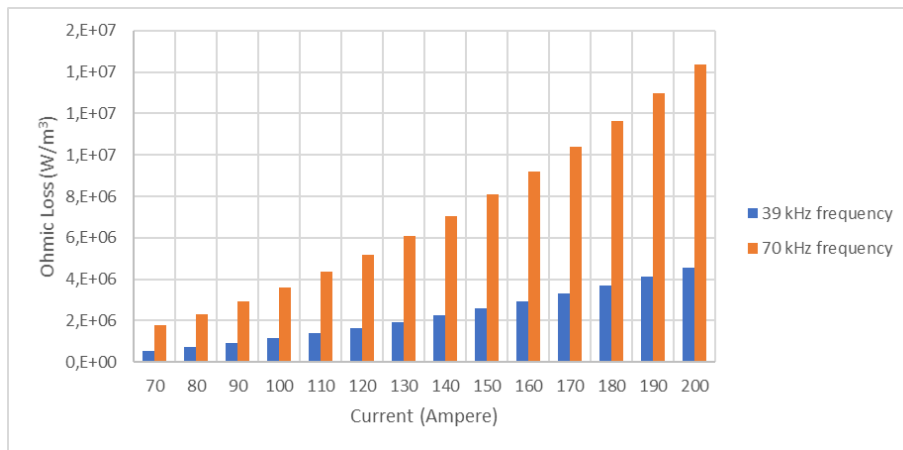


Fig. 14. The maximum value of the ohmic loss in all variations

4.2 Thermal Analysis

As elaborated in the methodology, two phases of the simulation were carried out to analyze the temperature distribution around inductive asphalt. The process of transferring data was done by ANSYS Workbench. Ohmic loss data is converted being internal heat generation and distributed by conduction. As shown in Figure 15, it can be seen that heat generated comes from the same area as the high ohmic loss area. The generated heat will be concentrated in this area before being transferred along its body in the conduction process.

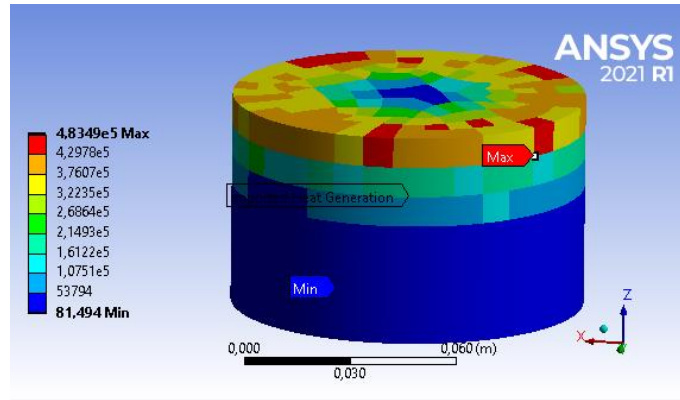


Fig. 15. Heat generation in inductive asphalt

In this study, thermal analysis has been simulated using the transient model. So, the change in thermal can be observed over time. Figure 16 shows the temperature distribution of inductive asphalt at the first 900 s. It can be seen that the highest temperature reaches 93 °C at the top surface, and the lowest temperature hits 38 °C at the bottom surface. Due to the low thermal conductivity, heat is difficult to spread evenly throughout the asphalt body.

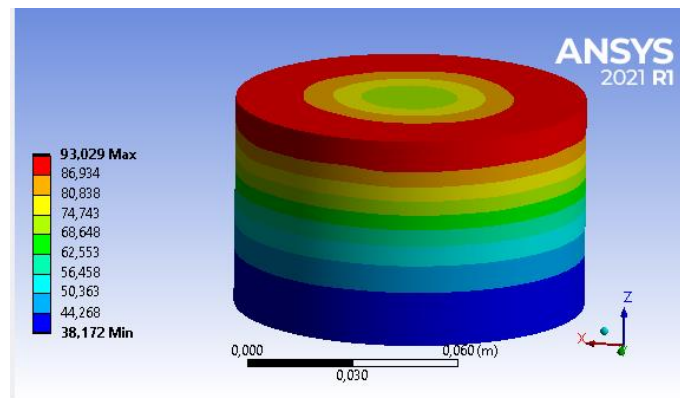


Fig. 16. Temperature distribution in inductive asphalt at first 900 s

As mentioned in the methodology, a comparison between experimental and numerical was carried out. Figure 17 shows the temperature profile of the inductive asphalt after being heated for 6 and 10 minutes. It can be seen that the high temperatures are concentrated on the top surface of the sample before being transferred along its body.

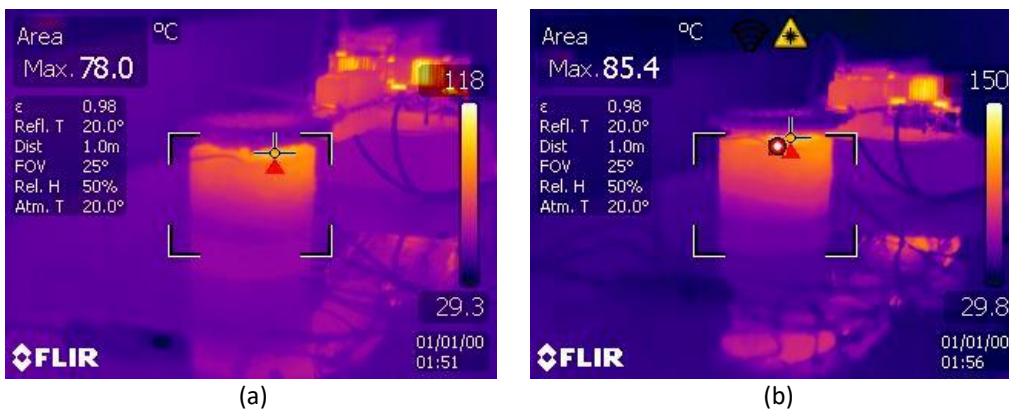


Fig. 17. Temperature profile after being heated for (a) 6 minutes (b) 10 minutes

Figure 18 shows the comparison between experimental and numerical results for 70 Ampere current with 39 kHz frequency. It can be seen that the error between experimental and numerical data is below 8,5%. The difference value could be due to differences in boundary conditions where it was possible. The asphalt sample could have a slightly different property because of the mixing method of additional materials.

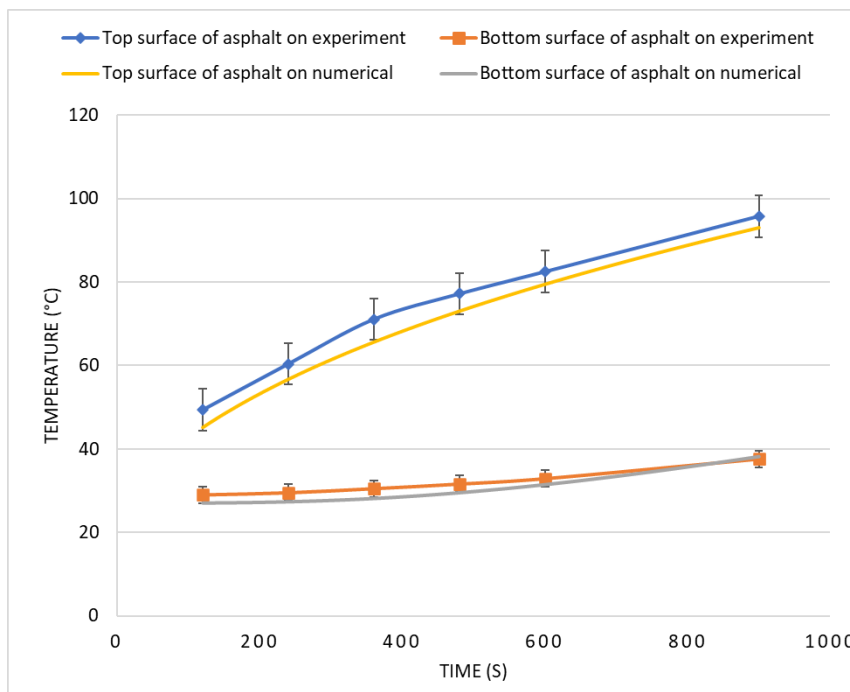


Fig. 18. Comparison between the experimental and numerical results of temperature distribution

The difference in current and frequency used to affect the heating speed and temperature distribution of the inductive asphalt. All models and parameters that are used are consistent with the experimental model that has been done previously. Then, using the exact modeling and simulation procedures, two frequency setups of 39 and 70 kHz are used. The current was also variated, starting with 70 until 200 Ampere.

Figure 19 shows the comparison data of temperature and the current flowing in the coil with a 39 kHz frequency. The higher current generates a higher temperature at a certain period. The self-healing phase (at 80 °C) cannot be reached at the first 20 s on any current magnitude. Variations of 190 Ampere and 200 Ampere can achieve 80 °C on the asphalt surface at the first 40 s. Although these variations can reach the target temperature quickly, the power required is greater and costs more as a consequence. The lower current needs longer times to reach this temperature, such as 160 Ampere variation that will reach the target temperature at the first 60 s or 120 Ampere variation that will reach it at the first 120 s. The lower currents do not require high power and are also cheaper, but they will take a longer time.

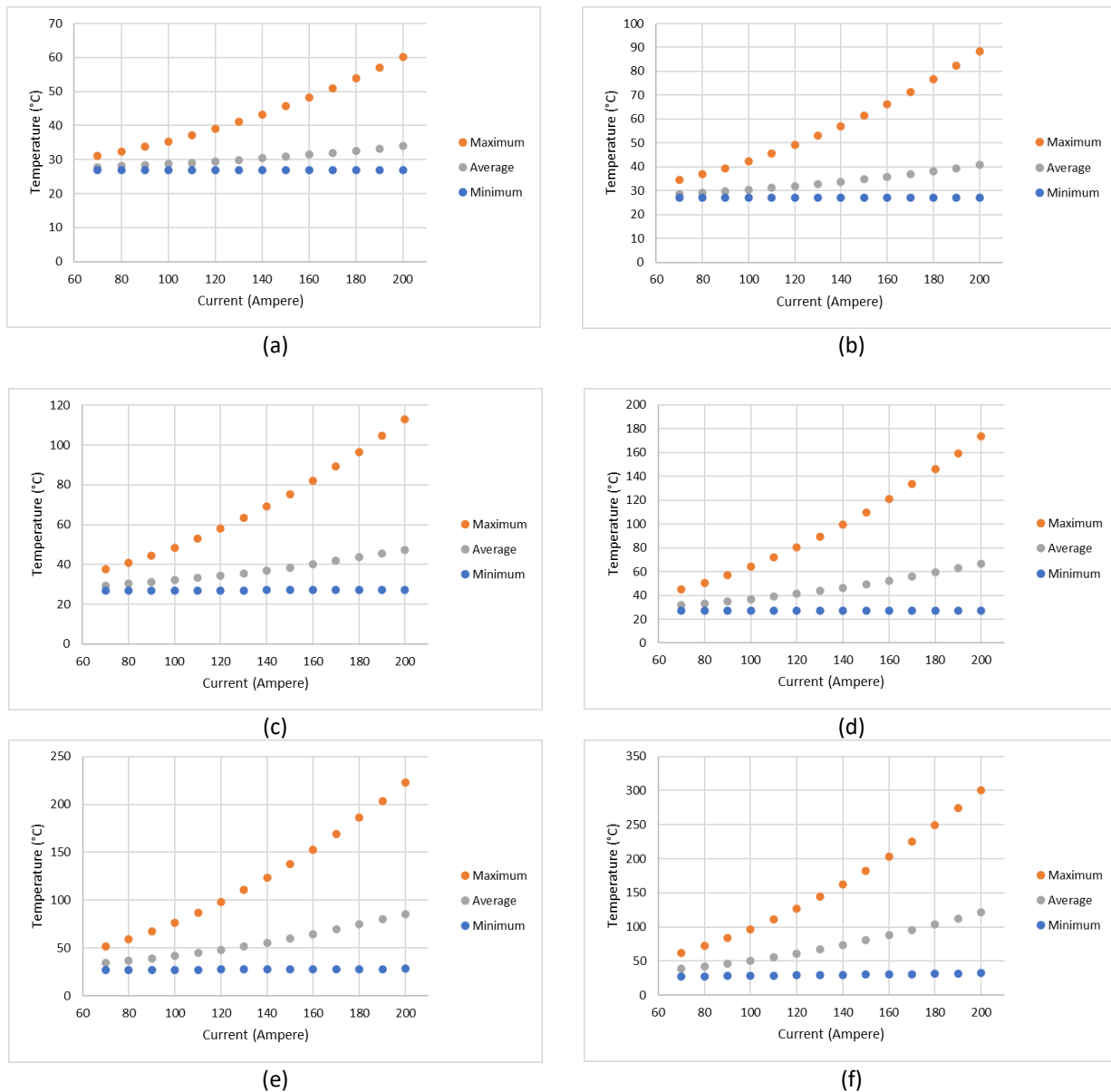


Fig. 19. Comparison of current and temperature distribution of induction heating on inductive asphalt with a 39 kHz frequency (a) at first 20 s (b) at first 40 s (c) at first 60 s (d) at first 120 s (e) at first 180 s (f) at first 300s

Figure 20 shows the same comparison as before with a 70 kHz frequency. As previously analyzed, higher frequencies produce larger electromagnetic fields, affecting the heat generated to be higher. With the use of a 70 kHz frequency, reaching 80 °C in the first 20 s only requires a current of 150 Ampere. It is much smaller than the current is needed before. This is because higher frequency requires a lower period of current oscillation and produces a stronger electromagnetic field around the coil, thereby maximizing the ohmic loss that occurs. Making an induction heater with a high frequency also requires a higher cost, but the effect can reduce the power needed with the same heating result.

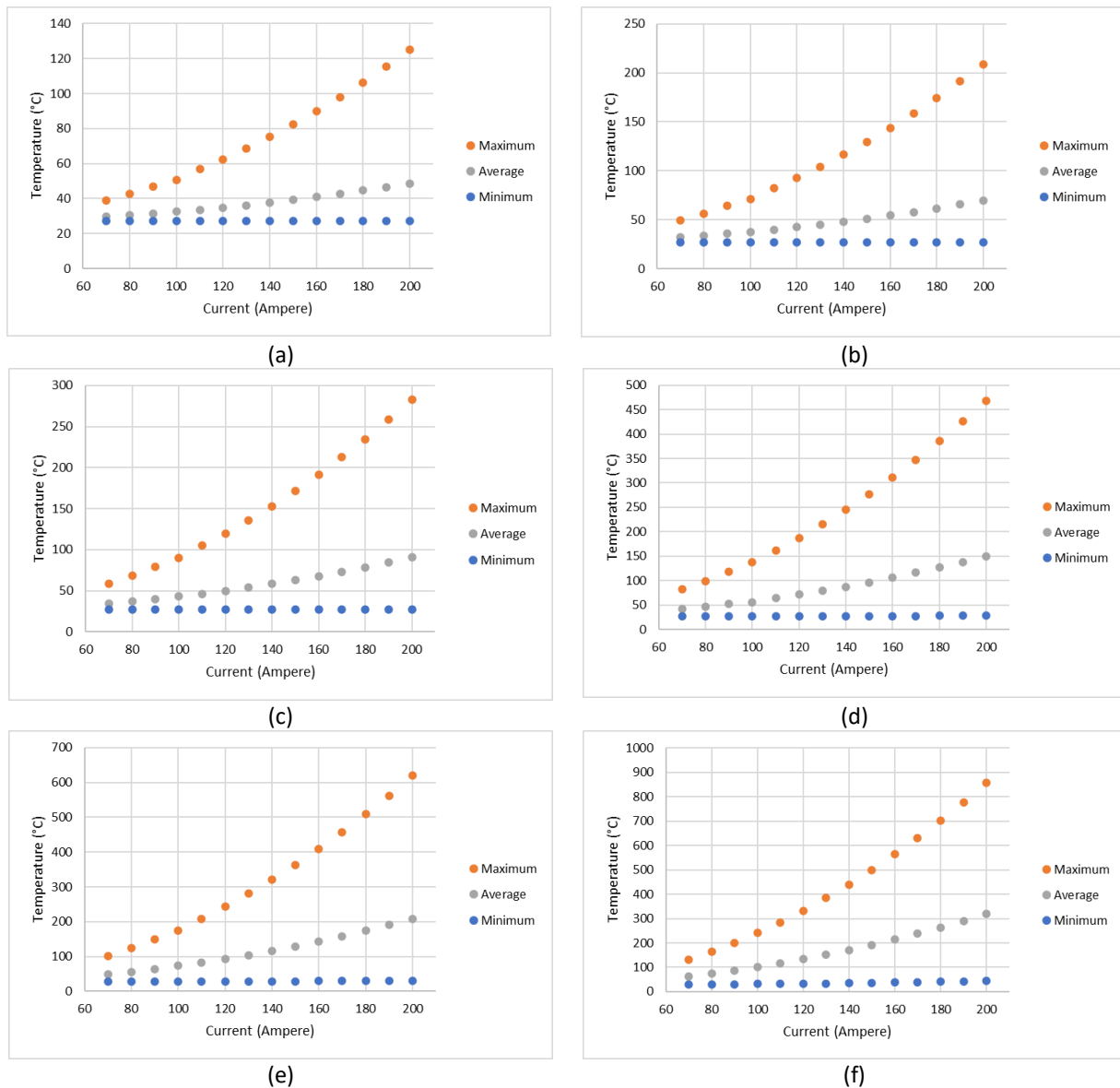


Fig. 20. Comparison of current and temperature distribution of induction heating on inductive asphalt with a 70 kHz frequency (a) at first 20 s (b) at first 40 s (c) at first 60 s (d) at first 120 s (e) at first 180 s (f) at first 300s

5. Conclusion

This study has proved that induction heating on asphalt can be applied as a technique to reach the self-healing phase. Simulations were carried out using current and frequency variations. Considering all the factors, we draw the following conclusions:

- I. Due to the low thermal conductivity, high temperature is concentrated on the top surface of the asphalt and does not conduct to the bottom of the asphalt. This cause only the top of the asphalt to melt and become Newtonian fluid. To melt the bottom of the asphalt, a very high temperature is required at the top, which will damage the asphalt itself.
- II. Overall, this condition can overcome microcracks on the surface, but not enough to heal the cracks or gaps that occur in the deeper parts.
- III. Some variations are considered less efficient for heating because it takes time too long. The result shows a higher frequency can produce more heat on the same current.

- IV. A higher current and frequency lead to higher heat as well, but the cost efficiency needs to be considered as the required temperature only needs to be up to 80 °C.

More research is needed to create inductive asphalt that is easier to be heated by induction heating so that the high temperature is not concentrated on the surface only.

Acknowledgment

Authors acknowledge Universitas Sebelas Maret through financial support under Hibah PNPB 2022, LPPM UNS. We also thank PT HK Aston for the bitumen material support.

References

- [1] Xu, Shi, Alvaro García, Junfeng Su, Quantao Liu, Amir Tabaković, and Erik Schlangen. "Self-Healing Asphalt Review: From Idea to Practice." *Advanced Materials Interfaces* 5, no. 17 (2018): 1800536. <http://doi.org/10.1002/admi.201800536>
- [2] Menozzi, Alessandro, Alvaro Garcia, Manfred N. Partl, Gabriele Tebaldi, and Philipp Schuetz. "Induction healing of fatigue damage in asphalt test samples." *Construction and Building Materials* 74 (2015): 162-168. <http://doi.org/10.1016/j.conbuildmat.2014.10.034>
- [3] García, Álvaro, Erik Schlangen, Martin van de Ven, and Dave van Vliet. "Induction heating of mastic containing conductive fibric and fillers." *Materials and structures* 44, no. 2 (2011): 499-508. <http://doi.org/10.1617/s11527-010-9644-2>
- [4] Hamdi, H., Sigit P. Hadiwardoyo, A. Gomes Correia, and Paulo AA Pereira. "Pavement maintenance optimization strategies for national road network in Indonesia applying genetic algorithm." (2017). <http://doi.org/10.1016/j.proeng.2017.11.074>
- [5] Garcia, A., S. Salih, and B. Gómez-Meijide. "Optimum moment to heal cracks in asphalt roads by means electromagnetic induction." *Construction and Building Materials* 238 (2020): 117627. <http://doi.org/10.1016/j.conbuildmat.2019.117627>
- [6] Ahsan, Qumrul, Wong Teng Hui, Intan Sharhida Othman, Liew Pay Jun, and Azma Putra. "Preparation and Characterization of Natural Fiber Filled Asphalt Based Damping Material." *Journal of Advanced Research in Fluid Mechanics and Thermal Sciences* 47, no. 1 (2018): 8-15.
- [7] Aziz, Siti Aishah Abdul, Saiful Amri Mazlan, Nik I. Nik Ismail, Seung-Bok Choi, and N. A. Yunus. "An enhancement of mechanical and rheological properties of magnetorheological elastomer with multiwall carbon nanotubes." *J. Intell. Mater. Syst. Struct.* 28, no. 20 (2017): 3127-3138. <http://doi.org/10.1177/1045389x17705211>
- [8] Ghosh, Swapan Kumar, ed. *Self-healing materials: fundamentals, design strategies, and applications*. Vol. 18. Weinheim: Wiley-vch, 2009. <https://doi.org/10.1002/9783527625376>
- [9] Ayar, Pooyan, Fernando Moreno-Navarro, and M^a Carmen Rubio-Gámez. "The healing capability of asphalt pavements: a state of the art review." *Journal of Cleaner Production* 113 (2016): 28-40. <http://doi.org/10.1016/j.jclepro.2015.12.034>
- [10] Concha, Jose L., and Jose Norambuena-Contreras. "Thermophysical properties and heating performance of self-healing asphalt mixture with fibres and its application as a solar collector." *Applied Thermal Engineering* 178 (2020): 115632. <http://doi.org/10.1016/j.applthermaleng.2020.115632>
- [11] Garcia, Alvaro, Erik Schlangen, and Martin Van de Ven. "Two ways of closing cracks on asphalt concrete pavements: microcapsules and induction heating." In *Key Engineering Materials*, vol. 417, pp. 573-576. Trans Tech Publications Ltd, 2010. <http://doi.org/10.4028/www.scientific.net/KEM.417-418.573>
- [12] Liu, Quantao, Wan Yu, Erik Schlangen, and Gerbert van Bochove. "Unravelling porous asphalt concrete with induction heating." *Construction and Building Materials* 71 (2014): 152-157. <http://doi.org/10.1016/j.conbuildmat.2014.08.048>
- [13] Liu, Quantao. *Induction Healing of Porous Asphalt Concrete*. S.l.: s.n., 2012.
- [14] Liu, Kai, Chaoliang Fu, Peixin Xu, Shuqin Li, and Muyang Huang. "An eco-friendliness inductive asphalt mixture comprising waste steel shavings and waste ferrites." *Journal of Cleaner Production* 283 (2021): 124639. <http://doi.org/10.1016/j.jclepro.2020.124639>
- [15] Garcia, Alvaro, Moisés Bueno, José Norambuena-Contreras, Quantao Liu, and Manfred N. Partl. "The model for induction-healing asphalt concrete." *Asphalt Pavements* 1 (2014): 1431-1440. <http://doi.org/10.1201/b17219>
- [16] Gómez-Meijide, Breixo, Harith Ajam, Alvaro Garcia, and Stefan Vansteenkiste. "Effect of bitumen properties in the induction healing capacity of asphalt mixes." *Construction and Building Materials* 190 (2018): 131-139. <http://doi.org/10.1016/j.conbuildmat.2018.09.102>

- [17] García, Álvaro. "Self-healing of open cracks in asphalt mastic." *Fuel* 93 (2012): 264-272. <http://doi.org/10.1016/j.fuel.2011.09.009>
- [18] Grossegger, D., and A. Garcia. "Influence of the thermal expansion of bitumen on asphalt self-healing." *Applied Thermal Engineering* 156 (2019): 23-33. <http://doi.org/10.1016/j.applthermaleng.2019.04.034>
- [19] Grossegger, D., B. Gomez-Meijide, S. Vansteenkiste, and A. Garcia. "Influence of rheological and physical bitumen properties on heat-induced self-healing of asphalt mastic beams." *Construction and Building Materials* 182 (2018): 298-308. <http://doi.org/10.1016/j.conbuildmat.2018.06.148>
- [20] García, Álvaro, Erik Schlangen, and Martin Van de Ven. "Properties of capsules containing rejuvenators for their use in asphalt concrete." *Fuel* 90, no. 2 (2011): 583-591. <http://doi.org/10.1016/j.fuel.2010.09.033>
- [21] Anupam, B. R., Umesh Chandra Sahoo, and Anush K. Chandrappa. "A methodological review on self-healing asphalt pavements." *Construction and Building Materials* 321 (2022): 126395. <https://doi.org/10.1016/j.conbuildmat.2022.126395>
- [22] Sun, Daquan, Guoqiang Sun, Xingyi Zhu, Alvaro Guarin, Bin Li, Ziwei Dai, and Jianming Ling. "A comprehensive review on self-healing of asphalt materials: Mechanism, model, characterization and enhancement." *Advances in colloid and interface science* 256 (2018): 65-93. <https://doi.org/10.1016/j.cis.2018.05.003>
- [23] Karimi, Mohammad M., Saeed Amani, Hamid Jahanbakhsh, Behnam Jahangiri, and Amir H. Alavi. "Induced heating-healing of conductive asphalt concrete as a sustainable repairing technique: A review." *Cleaner Engineering and Technology* 4 (2021): 100188. <http://doi.org/10.1016/j.clet.2021.100188>
- [24] Pokaad, Alif Zulfakar Bin, Khisbullah Hudha, and Mohd Zakaria Bin Mohamad Nasir. "Simulation and experimental studies on the behaviour of a magnetorheological damper under impact loading." *International Journal of Structural Engineering* 2, no. 2 (2011): 164-187. <https://doi.org/10.1504/IJSTRUCTE.2011.039422>
- [25] Vishnuram, Pradeep, Gunabalan Ramachandiran, Thanikanti Sudhakar Babu, and Benedetto Nastasi. "Induction Heating in Domestic Cooking and Industrial Melting Applications: A Systematic Review on Modelling, Converter Topologies and Control Schemes." *Energies* 14, no. 20 (2021): 6634. <http://doi.org/10.3390/en14206634>
- [26] Lucía, Oscar, Pascal Maussion, Enrique J. Dede, and José M. Burdío. "Induction heating technology and its applications: past developments, current technology, and future challenges." *IEEE Transactions on industrial electronics* 61, no. 5 (2013): 2509-2520. <http://doi.org/10.1109/tie.2013.2281162>
- [27] El-Mashad, Hamed M., and Zhongli Pan. "Application of induction heating in food processing and cooking." *Food Engineering Reviews* 9, no. 2 (2017): 82-90. <http://doi.org/10.1007/s12393-016-9156-0>
- [28] Mohamad, N., S. A. Mazlan, Fitriani Imaduddin, Seung-Bok Choi, and I. I. M. Yazid. "A comparative work on the magnetic field-dependent properties of plate-like and spherical iron particle-based magnetorheological grease." *PLoS one* 13, no. 4 (2018): e0191795. <http://doi.org/10.1371/journal.pone.0191795>
- [29] Rudnev, Valery, Don Loveless, and Raymond L. Cook. *Handbook of induction heating*. CRC press, 2017. <http://doi.org/10.1201/9781315117485-3>
- [30] Sun, Rui, Yongjun Shi, Zhengfu Pei, Qi Li, and Ruihai Wang. "Heat transfer and temperature distribution during high-frequency induction cladding of 45 steel plate." *Applied Thermal Engineering* 139 (2018): 1-10. <http://doi.org/10.1016/j.applthermaleng.2018.04.100>
- [31] Ismail, Ahmad Rasdan, Norfadzilah Jusoh, Raemy Md Zein, Ismail Abdul Rahman, Mohd Amin Mahd Asri, and Nor Kamilah Makhtar. "Application of computational fluid dynamic simulation for the study of heat stress and heat strain-A review." *Journal of Advanced Research in Fluid Mechanics and Thermal Sciences* 73, no. 2 (2020): 138-145. <https://doi.org/10.37934/arfmts.73.2.138145>
- [32] Alkassasbeh, Hamzeh. "Numerical solution of heat transfer flow of casson hybrid nanofluid over vertical stretching sheet with magnetic field effect." *CFD Letters* 14, no. 3 (2022): 39-52. <https://doi.org/10.37934/cfdl.14.3.3952>
- [33] García, Álvaro, Erik Schlangen, Martin van de Ven, and Quantao Liu. "A simple model to define induction heating in asphalt mastic." *Construction and Building Materials* 31 (2012): 38-46. <http://doi.org/10.1016/j.conbuildmat.2011.12.046>
- [34] Li, Hechuan, Jianying Yu, Quantao Liu, Yuanyuan Li, Yaqi Wu, and Haiqin Xu. "Induction heating and healing behaviors of asphalt concretes doped with different conductive additives." *Advances in Materials Science and Engineering* 2019 (2019). <http://doi.org/10.1155/2019/2190627>
- [35] Apostolidis, P. A. N. O. S. "Experimental and numerical investigation of induction heating in asphalt mixes." (2015). <http://doi.org/10.13140/RG.2.2.20606.28480>
- [36] Imaduddin, Fitriani, Saiful Amri Mazlan, Hairi Zamzuri, and Abdul Yasser Abd Fatah. "Testing and parametric modeling of magnetorheological valve with meandering flow path." *Nonlinear Dynamics* 85, no. 1 (2016): 287-302. <http://doi.org/10.1007/s11071-016-2684-6>
- [37] Pranoto, Setyo, Bhre Wangsa Lenggana, Eko Prasetya Budiana, and Agung Tri Wijayanta. "Fluid Flow Analysis at Single and Dual Plenum Intake Manifolds to Reduce Pressure Drops Using Computational Approach." *Journal of*

Advanced Research in Fluid Mechanics and Thermal Sciences 97, no. 1 (2022): 1-12.
<https://doi.org/10.37934/arfmts.97.1.112>